

NOTE

Red, Gray, and Blue: Near Infrared Spectrophotometry of Faint Moons of Uranus and Neptune

David E. Trilling^{1,2}*UCO/Lick Observatory, University of California, Santa Cruz, California 95064*E-mail: trilling@ucolick.org

and

Robert H. Brown¹*Lunar and Planetary Laboratory and Steward Observatory, University of Arizona, Tucson, Arizona 85721*

Received March 2, 2000; revised July 24, 2000

Using the CoCo Cold Coronagraph at NASA's Infrared Telescope Facility on Mauna Kea, we observed the uranian satellites Miranda, Puck, Portia, and Rosalind and the neptunian satellite Proteus in the near infrared (JHK) to determine the albedos of those faint satellites. In V-J, all of Puck, Portia, Rosalind, and Proteus are very blue, similar to the colors of many icy satellites and of water ice. The satellites we observed have a wide range of J-H colors, with Miranda being blue, Proteus being gray, and Puck, Portia, and Rosalind being red. For the satellites for which we could determine H-K (Miranda, Puck, and Proteus), the colors are gray to red. As a whole, spectrally, these five satellites lie between icy Solar System satellites (e.g., saturnian satellites or the major uranian satellites) and Kuiper belt objects. The redness of Proteus and Puck and perhaps other satellites suggests the presence of organic material, although the redness is also similar to that of C- and D-class asteroids and some outer jovian moons. In all cases, diagnostic spectral features could be masked by broadband photometry. © 2000 Academic Press

Key Words: satellites of Uranus; satellites of Neptune; infrared observations; spectrophotometry; ices.

1. Previous observations. The outer planets Uranus and Neptune each have a flock of small, faint satellites, many of which have been seen only once, during Voyager encounters (Smith *et al.* 1986, 1989). We observed five faint satellites of these planets in the near-infrared from Mauna Kea: Miranda (UV), the smallest of the pre-Voyager uranian moons; Puck (UXV), the largest of the uranian Voyager moons; Portia (UXII), the second largest uranian Voyager moon; Rosalind (UXIII), another Voyager moon; and Proteus (NVIII), the largest

of the neptunian Voyager satellites (Kuiper 1949; Smith *et al.* 1986, 1989). Our observations of Miranda were serendipitous in that Miranda was relatively close to the planet during our first epoch uranian observations; this allowed us to compare our photometry to the most complete near infrared dataset on that moon, that of Baines *et al.* (1998). Puck has been detected from the ground twice before: at K-band with adaptive optics at the Canada–France–Hawaii Telescope (CFHT) on Mauna Kea (Roddier *et al.* 1997a) and in JHK with adaptive optics at the European Southern Observatory (ESO) at La Silla, Chile (Marchis *et al.* 1999). Puck has also been observed in BVRI by Pascu *et al.* (1995, 1998a,b) and several other filters at $\lambda < 1$ micron (Karkoschka 1997) with the Hubble Space Telescope (HST). Portia has not been seen from the ground before, only from HST in the visible (Storrs *et al.* 1996) and near infrared (I band) (Pascu *et al.* 1995). Likewise, Rosalind has not been seen from the ground before, only from HST in BVRI (Pascu *et al.* 1998b). Proteus was first detected from the ground at ESO in 1992 at $0.8 \mu\text{m}$ (Colas and Buil 1992), and later in the near-infrared with adaptive optics from CFHT (Roddier *et al.* 1997a,b, 1998a,b; Sicardy *et al.* 1999), as well as from HST in the visible (Pascu *et al.* 1998a) and near infrared (Terile *et al.* 1998; Dumas *et al.* 1999). The present work is the first time that JHK observations have been reported for Puck, Portia, Rosalind, and Proteus, although we have only upper limits for the reflectance of Portia and Rosalind in K-band. Since we know the physical sizes of these satellites from the Voyager measurements, we can determine the near infrared albedos for these small, faint satellites. In Section 3, we compare the near-IR colors we have acquired to those of other Solar System bodies and laboratory analogs and discuss some implications of the varied near infrared colors.

2. Our observations and results. We observed the uranian system on 9 and 10 September 1999 and the neptunian system on 7 and 8 September 1999 at NASA's Infrared Telescope Facility (IRTF) on Mauna Kea; we observed the uranian system at a phase angle of 1.56° and the neptunian system at a phase angle of 1.29° . We observed each system at J, H, and K bands (central wavelengths of 1.26, 1.62, and $2.21 \mu\text{m}$, respectively) using CoCo, the Cold Coronagraph (Wang *et al.* 1994; Toomey *et al.* 1998). CoCo is a cryogenically cooled Lyot coronagraphic front end to the IRTF's facility infrared camera NSFCAM (Rayner *et al.* 1993; Shure *et al.* 1994) and has gaussian apodized focal plane masks and a cooled articulatable pupil plane mask to block light from the central object and reduce scattered light in the near-planet (or near-star) environment. CoCo has a small field of view (14×14 arcsec) and uses the 0.055 arcsec per pixel plate scale. Additionally, since CoCo allows focal plane masks of various sizes, we were able to use masks of nearly the angular diameters of the planets

¹ Visiting Astronomer at the Infrared Telescope Facility, which is operated by the University of Hawaii under contract to the National Aeronautics and Space Administration.

² Present address: University of Pennsylvania, David Rittenhouse Laboratory, 209 S. 33rd Street, Philadelphia, Pennsylvania 19104. E-mail: trilling@hep.upenn.edu.

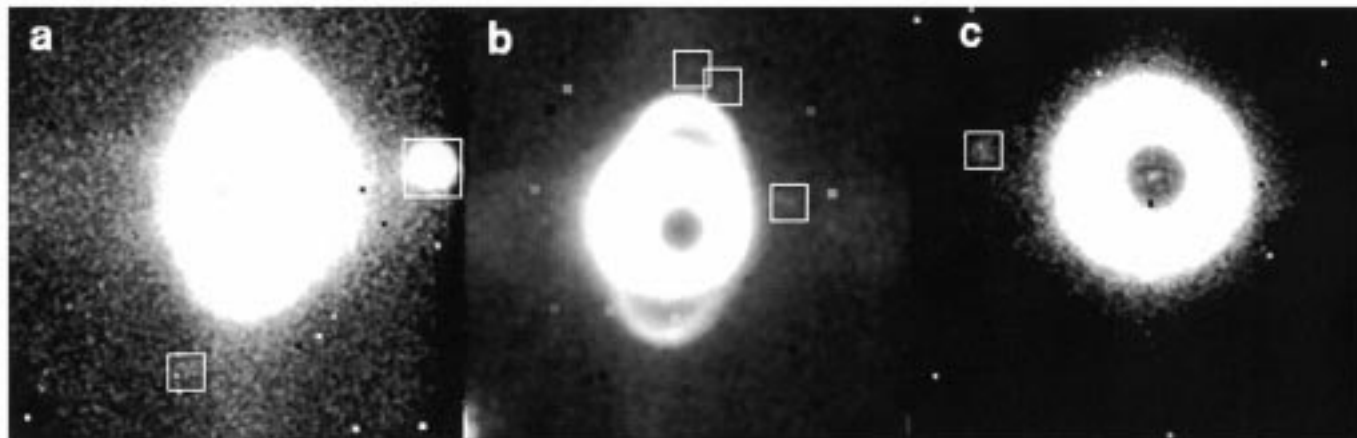


FIG. 1. Images of faint satellites of Uranus and Neptune. North is up and East is left. Panel (a) shows Uranus, Miranda (box to the right), and Puck (lower left box). Panel (b) shows Uranus, Puck (box due west), Portia (northwest box), and Rosalind (box nearly due north). Panel (c) shows Neptune and Proteus (box due east). The moon Ariel (UI) is just off the frame of panel (b) to the lower left (bright spot at the edge of the frame). All images are in J band, and are 300-s exposures, with 300-s sky frames subtracted. The field of view is $14'' \times 14''$. Each image has been boxcar smoothed with a 3×3 box. The stretch is different on each image, to accentuate the rings and satellites. The focal plane masks are $3.7''$ and $2.7''$ in diameter for Uranus and Neptune, respectively, and can be seen in the center of the planets' disks in panels (b) and (c). For panel (a), the mask is also present but a slight misalignment of the mask and planet allowed some scattered light to dominate the center of the planet's disk in this stretch. The epochs for the observations are panel (a), 1999 SEP 09 07:46 UT; panel (b), 1999 SEP 10 08:08 UT; and panel (c), 1999 SEP 08 09:03 UT (starting times for the 300-s on-source integrations).

in question for maximum light rejection (3.7 and 2.7 arcsec for Uranus and Neptune, respectively).

Detecting these faint satellites was possible by using the known ephemeris from the JPL Horizons Web page² and—in some cases—by making a movie of a series of images and looking for faint objects executing orbital motion. Observations which included Miranda were short enough so that Miranda was not saturated in the images. Puck and Proteus were easily detected in all cases; Portia and Rosalind were more difficult observations. The chief problems in measuring the magnitudes of these faint satellites of Uranus and Neptune are the scattered light field from the planets and the moons' large angular motions on the sky. To address the former problem, we removed the background with a bilinear fit to the scattered light from the planet. This fit was based on measuring the scattered light background in all directions around the satellite at a distance of 0.5 arcsec, the size of the seeing disk. The effective photometric aperture was around 0.5 arcsec radius except for Miranda, for which we used a 1 -arcsec radius; at larger radii, noise or scattered light became the dominant flux sources with increasing annuli. We observed each satellite typically at least three times per night per filter (individual exposures were 5 min), and the error bars reported in this work represent the standard deviation obtained from these independent measurements. This background removal technique works reasonably well, especially for the brighter satellites, but difficulties in subtracting the steeply varying background dominate the scatter in the measurements of the fainter satellites.

Because of the satellites' large angular motions, five minute integrations were the maximum duration possible to retain satellites within one seeing disk (typically 0.5 arcseconds). Thus, we imaged in a series of five minute integrations, rotating through J, H, and K bands, and the faint Elias standard star SAO126618 (Elias *et al.* 1982) at the same airmass as the satellite observations were made. For each five minute object integration, we also obtained a five minute sky exposure. We observed object–sky pairs in each of the three filters typically three times per night. We observed the satellites at hour angles of $00:00$ to $01:30$, at airmasses of 1.256 to 1.834 . Our stellar photometry measurements have scatter of 1 – 2% ; all magnitudes and colors reported are in the Elias–CIT standard bandpasses. All of the magnitudes and albedos we report are for disk-integrated observations of these satellites. The central sub-Earth longitudes we observed,

for the first and second observations of each satellite, are the following: 187 – 207 for Miranda (9 Sep 1999 only); 67 – 131 and 192 – 249 for Puck; 246 – 340 and 246 – 330 for Portia; 276 – 353 for Rosalind (10 Sep 1999 only); and 113 – 147 and 81 – 105 for Proteus. (The trailing hemisphere is centered on 90° the leading hemisphere is centered on 270° .) The values presented here are averages of all observations, and ignore any possible spatial inhomogeneities.

Figure 1 shows images of these five faint moons. Panel (a) shows Uranus, with the moons Miranda and Puck; panel (b) shows Uranus with Puck, Portia, and Rosalind; and panel (c) shows Neptune with Proteus. The rings of Uranus can easily be seen in panels (a) and (b), but we did not detect the rings or ring arcs of Neptune. Each of these images represents a 5 -min integration on the planet, with a 5 -min sky frame subtracted from it. We detected Miranda, Proteus, and Puck in all of J, H, and K, and Portia and Rosalind in J and H. Typical separations from the limbs of the planets for our observations were 3.5 arcsec for Miranda and Proteus, 3 arcsec for Rosalind, and 2.5 arcsec for Portia and Puck. The surface brightnesses for Uranus and Neptune were approximately 8.27 and 9.43 visual magnitudes per square arcsecond.

TABLE 1
Visible–Near Infrared Colors of Faint Moons and Rings

	V-J	J-H	H-K
Miranda	0.99 ± 0.10	0.01 ± 0.10	-0.06 ± 0.13
Puck	-0.2 ± 0.4	0.5 ± 0.5	0.4 ± 0.6
Portia	0.3 ± 0.6	1.1 ± 0.6	< -0.1
Rosalind	0.0 ± 0.5	1.2 ± 0.6	< 1.1
Uranian rings	0.23 ± 0.15	0.32 ± 0.15	0.22 ± 0.15
Proteus	0.3 ± 0.2	0.5 ± 0.3	0.6 ± 0.4
Sun	1.11	0.34	0.02

Note. Faint moon V magnitudes are Miranda, 16.33 ± 0.07 , opposition magnitude (Veverka *et al.* 1987); Puck, 20.4 ± 0.3 , opposition magnitude (Thomas *et al.* 1989); Portia, 21.2 ± 0.3 , opposition magnitude (Thomas *et al.* 1989); Rosalind, 22.5 ± 0.3 , opposition magnitude (Thomas *et al.* 1989); and Proteus, 20.27 ± 0.04 , derived from Thomas *et al.* (1995), Thomas and Veverka (1991). Solar colors are from Colina *et al.* (1996).

² <http://ssd.jpl.nasa.gov/horizons.html>.

TABLE 2
Percent Albedos of Faint Moons and Rings

Body	V	J	H	K
Miranda	34 ± 2^a	30.2 ± 1.5	22.5 ± 1.6	20.5 ± 2.3
Puck	11 ± 1.5^b	2.0 ± 0.6	2.3 ± 0.9	3.6 ± 1.8
Portia	7.0 ± 2.1^c	3.3 ± 1.7	7.3 ± 3.7	<6.5
Rosalind	7.6 ± 0.8^c	2.6 ± 1.0	6.5 ± 2.6	<23
Proteus	6.2 ± 0.2^d	2.6 ± 0.5	2.8 ± 0.6	4.7 ± 1.4
N. Ring Ansa	6.1 ± 0.6^e	3.0 ± 0.3	2.7 ± 0.6	3.3 ± 0.7
S. Ring Ansa	6.1 ± 0.6^e	2.4 ± 0.2	2.5 ± 0.5	3.3 ± 0.7

Sources. (a) Geometric albedo (Veverka *et al.* 1987); (b) geometric albedo (Karkoschka 1997); (c) geometric albedo, derived from Thomas *et al.* (1989); (d) Thomas *et al.* (1995), Thomas and Veverka (1991); (e) geometric albedo of ring particles (Karkoschka 1997).

Note. Shown are our measured albedos of Miranda, Puck, Portia, Rosalind, and Proteus, and albedos of the north and south ring ansae, normalized to 3.3% at the K band, equal to the value from Baines *et al.* (1998). We used radii of 235 km for Miranda (Thomas 1988); 77 km, 55 km, and 29 km for Puck, Portia, and Rosalind, respectively (Thomas *et al.* 1989); and 210 km for Proteus (Thomas and Veverka 1991).

The results of our magnitude and albedo measurements are shown in Tables 1 and 2 and Fig. 2. We find that Miranda is relatively blue and bright (albedo 0.2–0.3). Puck, Portia, Rosalind, and Proteus are all dark (albedos less than 0.1). These four dark satellites are all blue in V-J. Proteus is gray in J-H and red in H-K; Puck, Portia, and Rosalind all are red in J-H and, where known, H-K. Our JHK magnitudes for Miranda are in very good agreement with those of Kesten *et al.* (1998) and Baines *et al.* (1998): Kesten *et al.* (1998) report JHK of 15.30 ± 0.05 , 15.14 ± 0.05 , and 15.40 ± 0.06 and Baines *et al.* (1998) report JHK of 15.67 ± 0.08 , 15.43 ± 0.05 , and 15.29 ± 0.04 , in comparison to our JHK of 15.34 ± 0.05 , 15.32 ± 0.07 , and 15.40 ± 0.11 . Our K magnitude for Proteus is 19.1 ± 0.3 , in very good agreement with the value of 19.0 ± 0.03 determined by Roddier *et al.* (1997b).

All satellites we detected were found within 0.5 arcsec of the predicted positions according to the JPL Horizons web page. We can therefore make no improvement on the orbital solutions and astrometry of these faint satellites.

We measured the ratio of surface brightness between the South and North ring ansae as 0.60 ± 0.06 , 0.70 ± 0.15 , and 0.75 ± 0.15 for J, H, and K, respectively. Baines *et al.* (1998) measured 0.940 ± 0.273 , 0.707 ± 0.144 , and 0.858 ± 0.035 in the same bandpasses. Our measurements agree to within the error bars; the opening angle of the rings changed slightly between their observations ($\sim 48^\circ$) and ours ($\sim 33^\circ$).

3. Discussion of colors and compositions. The errors on our measurements are dominated by subtracting the planets' scattered light from the near-satellite areas, producing error bars of 0.3 magnitudes or more in some cases. Furthermore, lightcurve effects have not been included: Thomas (1989) estimated that, for example, Puck's delta magnitude due to lightcurve effects can be at most 0.05 magnitudes; Karkoschka (1999) more recently has stated that lightcurve effects could be as large as 0.1 magnitudes for Portia and up to 0.3 magnitudes for Belinda, another small uranian moon. Because of our large error bars, and because of the inherently non-unique nature of broadband photometry, definitive comparisons between the observed moons and other Solar System bodies or laboratory spectra are impossible. However, we briefly point out some superficial similarities, and comment on the physical implications.

The colors of Miranda are most similar to other icy moons in the Solar System. Miranda's V-J, J-H, and H-K of 0.99 ± 0.10 , 0.01 ± 0.10 , and -0.06 ± 0.13 can be bracketed by the colors of the large, regular uranian moons Ariel (UI) and Umbriel (UII) (with colors 1.25 ± 0.20 , 0.23 ± 0.10 , and -0.07 ± 0.10 (Nicholson and Jones 1980; Cruikshank 1980)) and the saturnian moons Tethys (SIII) and Dione (SIV) (colors 0.85 ± 0.15 , -0.20 ± 0.15 , and -0.14 ± 0.15 (Cruikshank 1980)). All of these bodies, including Miranda, are known to have

water ice on their surfaces, and all of their reflectances are similar to laboratory spectra of water ice (Cruikshank and Brown 1981; Soifer *et al.* 1981; Fink *et al.* 1976; Brown and Clark 1984; Brown and Cruikshank 1997) (see Fig. 2). We confirm that Miranda is fainter than its larger fellow regular uranian satellite Ariel (cf. Baines *et al.* 1998).

The V-J colors of Portia, Proteus, Puck, and Rosalind are all bluer than solar. Whereas blue V-J seems to be uncommon in the Kuiper Belt (e.g., Davies *et al.* 2000), this relative decrease in reflectance from the visible to the near-infrared is typical of water ice, and is typical among icy satellites in the outer Solar System (e.g., Morrison *et al.* 1976, Cruikshank (1980)). Additionally, it is well known from laboratory measurements that pure water ice is very blue in V-J (e.g., Clark and Lucey 1984). Blue V-J for satellites may indicate the presence of water ice on these bodies.

Portia is blue in V-J and red in J-H. The upper limit on the K-band reflectance gives a slightly blue H-K, but because of the large error bars at H-band (0.5 mag), slightly red H-K cannot be ruled out. The best Solar System small body analogs for the red J-H (1.1 ± 0.6) and approximately neutral H-K (<-0.1) colors of Portia appear to be the Kuiper belt objects (KBOs) 1996 TP₆₆ (0.58 ± 0.10 , 0.10 ± 0.10) and 1996 TQ₆₆ (1.00 ± 0.10 , 0.03 ± 0.10). (Noll *et al.* 2000). Both of these KBOs could have near infrared water ice features up to 10% in depth, and the spectrophotometry of 1996 TQ₆₆ may indicate unidentified feature(s) (Noll *et al.* 2000). Many features less than 10–20% can be hidden in the broadband photometry of these two KBOs and, by implication, in Portia's colors too. All three of these objects are red in J-H, possibly indicating organic materials on their surfaces (see below).

Proteus is consistent with gray in J-H (0.5 ± 0.3) and is red in H-K (0.6 ± 0.4). A range of Solar System objects with various colors bracket Proteus' colors, from icy objects with blue J-H and red H-K to objects with modestly red J-H and H-K (see next section for discussion of objects with red J-H and H-K). Saturn's moon Phoebe (SIX) has J-H and H-K of 0.23 ± 0.14 and 0.41 ± 0.15 (Cruikshank 1980), though these values were later revised to 0.25 ± 0.15 and 0.15 ± 0.20 (Degewij *et al.* 1980). Jewitt and Luu (1998) report that the KBO 1996 TO₆₆ has J-H and H-K of -0.21 ± 0.17 and 0.81 ± 0.15 , though Noll *et al.* (2000) report a very different -0.17 ± 0.13 and -0.38 ± 0.15 . One explanation for the various K-band reflectances of this KBO is that it may have spatially heterogeneous surface water ice deposits. This possibility is also reflected in Phoebe, where the best model fit to spectral data uses only slightly more than 3% by weight water ice, compared to almost 97% amorphous carbon (Owen *et al.* 1999). Since both Phoebe and 1996 TO₆₆ are known to have water ice on their surfaces (Owen *et al.* 1999; Brown *et al.* 1999), in light of the color similarities with Proteus, it may be that Proteus also has water ice on its surface. The other body in the Solar System with strikingly blue J-H and red H-K is Jupiter's moon Sinope (JIX), with -0.109 and 0.653 (Sykes *et al.* 2000). Sinope has very different colors than its fellow jovian satellites, which potentially reflects a heterogeneous parent body (Sykes *et al.* 2000).

Puck is red in both J-H (0.5 ± 0.5) and H-K (0.4 ± 0.6), although because of the large error bars, blue J-H and H-K cannot be ruled out. As discussed above, the most likely surface material for blue JHK is water ice. However, Puck is nominally red in J-H and H-K, as is Rosalind (1.2 ± 0.6 , <1.1), and red JHK for Proteus also cannot be ruled out; perhaps this indicates similar surface compositions and geneses. It is surprising, therefore, that the small bodies in the Solar System with the most similar J-H and H-K likely formed much closer to the Sun: asteroid classes C and D (around 0.4 in J-H and 0.2 in H-K) (Hahn and Lagerkvist 1988) and five of Jupiter's outer satellites (around 0.5 in J-H and 0.2 in H-K_{short}) (Sykes *et al.* 2000). While it is easy to imagine that some of Jupiter's satellites are captured C- and D-asteroids (hence their spectral similarity), this does not seem a likely proposition for uranian or neptunian satellites. Instead, we look for analogs in the Solar System which, while less good matches, might imply more probable histories. The icy body which has the reddest known JHK is the Centaur 8405 Asbolus (formerly 1995 GO) (J-H = 0.40 ± 0.10 , H-K = 0.15 ± 0.10), which is likely covered with organic-rich molecules (Weintraub *et al.* 1997; Davies *et al.* 1998). Puck, Rosalind, and maybe Proteus might represent bodies which are similar to Asbolus, but redder, with more organic material (see below). Additionally, some water ice might be required for these bodies' blue V-J. In short, these three moons may have less

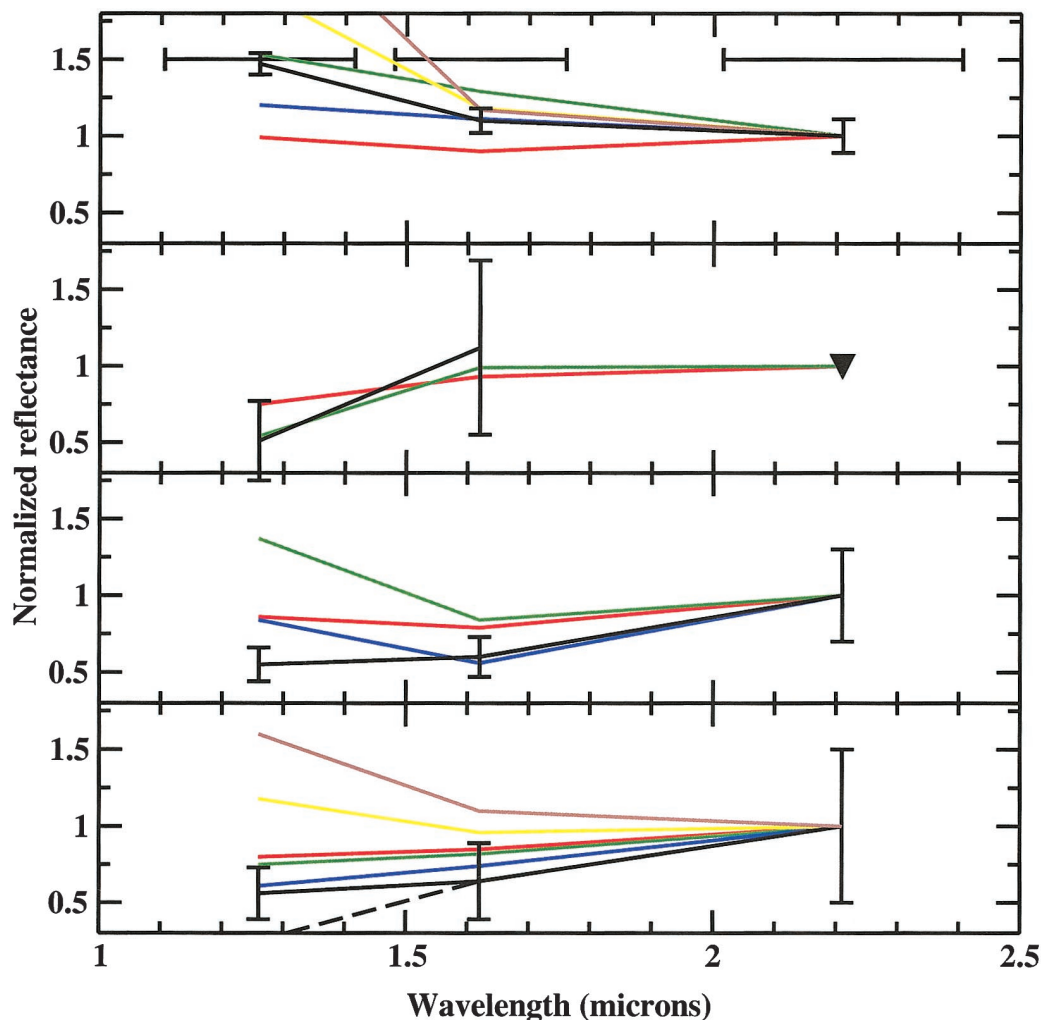


FIG. 2. Near infrared spectra of faint moons and comparison objects, normalized to unity at K-band. Panel (a): Miranda, black; Miranda, Baines *et al.* (1998), red; Miranda, Kesten *et al.* (1998), green; Umbriel, Cruikshank (1980), blue; Tethys, Cruikshank (1980), yellow; and water ice, Clark (1982), brown. Panel (b): Portia, including upper limit at K-band, black; 1996 TP₆₆, Noll *et al.* (2000), red; and 1996 TQ₆₆, Noll *et al.* (2000), green. Panel (c): Proteus, black; Phoebe, Cruikshank (1980) and Degewij *et al.* (1980), red; 1996 TO₆₆, average of Jewitt and Luu (1998), Brown *et al.* (1999), and Noll *et al.* (2000), green; and Sinope, Sykes *et al.* (2000), blue. Panel (d): Puck, black; Rosalind (J and H only), dashed black; C- and D-class asteroids, Hahn and Lagerkvist (1988), red; Asbolus, Weintraub *et al.* (1997), green; charcoal, Clark (1982) and Hartmann *et al.* (1982), blue; charcoal, Clark and Lucey (1984), yellow; and Mauna Kea soil with 1.0 wt.% ice, Clark and Lucey (1984), brown. Error bars are omitted for comparison objects, for clarity. The horizontal bars at the top of panel (a) show the bandpasses we used.

neutral material than other small, icy bodies, producing dynamic visible and near infrared colors.

The most likely cause of the red JHK slopes of these faint moons is organic-rich surface deposits: surfaces covered with heavy (long-chain) organics (molecules composed mainly of carbon and hydrogen) (Sagan *et al.* 1984; Cruikshank 1997). The redness of Puck, Rosalind, and potentially Portia and Proteus may indicate that a great deal of organic material is present. Many workers have shown that organic material can have very red slopes from the visible through 2 μm (e.g., Clark 1982; Hartmann *et al.* 1982; Bell *et al.* 1985; Andronico *et al.* 1987; Cloutis *et al.* 1994; Wilson *et al.* 1994; Moroz *et al.* 1998). In particular, combinations of clay, organics, charcoal, and coal are very red in VJHK (Clark 1982; Hartmann *et al.* 1982; Bell *et al.* 1985; Cloutis *et al.* 1994). Clark (1982) and Hartmann *et al.* (1982) found that fine-grained charcoal can produce red J-H (0.550) and H-K (0.353); however, this is not the best match for faint satellites because the charcoal's V-J (1.573) is much redder than the satellites' blue V-J. Clark *et al.* measured their charcoal to have a blue V-J (0.3042)

and J-H (0.1169) and a slightly red H-K (0.0686), similar in sense to the colors of Proteus (R. Clark, personal communication). Clark and Lucey (1984) have shown that combinations of charcoal and ice can produce spectra with slopes from blue to red in VJHK; combinations that are largely ice and >50 wt.% charcoal have a characteristic blue V-J (perhaps 40% decrease in reflectivity from V to J) and red JHK (perhaps 20% increase across this range) like the moons Puck, Rosalind, and maybe Portia and Proteus. The material "charcoal" used in these laboratory studies is not pure carbon and contains varying small amounts of hydrocarbons. The surfaces of these faint moons may be also covered with various combinations of materials like these laboratory analogs. Because radiolysis and photolysis of simple (short-chain) hydrocarbons produce long-chain hydrocarbons showing an increasingly large C/H ratio with dosage, it may be that the redness of these moons' spectra is due to the presence of complex organics on their surfaces. Proof of the presence of such compounds, however, must await higher quality and more detailed probes of the surface composition of these objects.

Compositional inferences made from color measurements are necessarily non-unique. Nevertheless, objects such as faint outer satellites, centaurs, and KBOs may fit generally into one of three broad categories: (1) blue objects such as Miranda which may have surfaces dominated by water ice; (2) objects with neutral colors (uranian rings) which may have spectrally neutral materials such as nearly pure, amorphous carbon present, or for which more complicated spectral signatures and compositions may be masked by broadband photometry; and (3) red objects such as Puck and Rosalind which might be objects whose surfaces are at least partially composed of heavy organics. Proteus and Portia may fit in any of these categories, depending on the values of their J-H colors. Despite color differences, we note that the bulk compositions of all of these bodies may be strikingly similar, with minor constituents producing large color variations. Additionally, most outer Solar System objects do not fit neatly into one of these three categories, indicating that more than one of these statements (and hence minor surface constituents) may apply. The faint moons studied here appear more similar as a group to KBOs than to any other group of Solar System small bodies. Thus, whether there are intrinsic and fundamental differences between the faint outer satellites, Kuiper belt objects, and centaurs is not clear. Naturally, additional data will assist in classification and lead toward understanding the formation of these outer Solar System icy satellites.

ACKNOWLEDGMENTS

It is our pleasure to thank Roger Clark and Dale Cruikshank for providing us with their near-infrared laboratory data. We also thank Andy Rivkin and Josh Emery for discussion and ideas, Christ Ftaclas for new CoCo masks, Doug Toomey for CoCo troubleshooting assistance, Dale Cruikshank for help with Kuiper's Miranda reference, Eugene Chiang for discussion about Uranus' rings, and telescope operators Paul Fukumura-Sawada and Dave Griep at the IRTF for their assistance with these observations. We thank referees Alex Storrs and John Davies for many useful suggestions. We made extensive use of the NASA Planetary Rings Node, JPL Horizons, and NASA ADS Web sites in this program. This work was supported by a NASA grant to RHB and grants to Doug Lin and Peter Bodenheimer.

REFERENCES

- Andronico, G., G. A. Baratta, F. Spinella, and G. Strazzulla 1987. Optical evolution of laboratory-produced organics: Applications to Phoebe, Iapetus, outer belt asteroids and cometary nuclei. *Astron. Astrophys.* **184**, 333–336.
- Baines, K. H., P. A. Yanamandra-Fisher, L. A. Lebofsky, T. W. Momary, W. Golisch, C. Kaminski, and W. J. Wild 1998. Near-infrared absolute photometric imaging of the uranian system. *Icarus* **132**, 266–284.
- Bell, J. F., D. P. Cruikshank, and M. J. Gaffey 1985. The composition and origin of the Iapetus dark material. *Icarus* **61**, 192–207.
- Brown, R. H., and R. N. Clark 1984. Surface of Miranda: Identification of water ice. *Icarus* **58**, 288–292.
- Brown, R. H., and D. P. Cruikshank 1997. Determination of the composition and state of icy surfaces in the outer solar system. *Annu. Rev. Earth. Planet. Sci.* **25**, 243–277.
- Brown, R. H., D. P. Cruikshank, and Y. Pendleton 1999. Water ice on the Kuiper belt object 1996 TO₆₆. *Astrophys. J.* **519**, L101–104.
- Clark, R. N. 1982. Implications of using broadband photometry for compositional remote sensing of icy objects. *Icarus* **49**, 244–257.
- Clark, R. N., and P. G. Lucey 1984. Spectral properties of ice–particulate mixtures and implications for remote sensing. 1. Intimate mixtures. *J. Geophys. Res.* **89**, 6341–6348.
- Cloutis, E. A., M. J. Gaffey, and T. F. Moslow 1994. Spectral reflectance properties of carbon-bearing minerals. *Icarus* **107**, 276–287.
- Colas, F., and C. Buil 1992. First Earth-based observations of Neptune's satellite Proteus. *Astron. Astrophys.* **262**, L13–14.
- Colina, L., R. C. Bohlin, and F. Castelli 1996. The 0.12–2.5 μm absolute flux distribution of the Sun for comparison with solar analog stars. *Astron. J.* **112**, 307–315.
- Cruikshank, D. P. 1980. Near-infrared studies of the satellites of Saturn and Uranus. *Icarus* **41**, 246–258.
- Cruikshank, D. P. 1997. Organic matter in the outer Solar System: From the meteorites to the Kuiper belt. In *From Stardust to Planetesimals* (Y. J. Pendleton and A. G. G. M. Tielens, Eds.), ASP Conference Series, Vol. 122, pp. 315–333, Astron. Soc. of the Pacific, San Francisco.
- Cruikshank, D. P. and R. H. Brown 1981. The uranian satellites: Water ice on Ariel and Umbriel. *Icarus* **45**, 605–611.
- Davies, J. K., N. McBride, S. L. Ellison, S. F. Green, and D. R. Ballantyne 1998. Visible and infrared photometry of six centaurs. *Icarus* **134**, 213–227.
- Davies, J. K., S. Green, N. McBride, E. Muzzerall, D. J. Tholen, R. J. Whiteley, M. J. Foster, and J. K. Hillier 2000. Visible and infrared photometry of fourteen Kuiper belt objects. *Icarus* **146**, 253–262.
- Degewij, J., D. P. Cruikshank, and W. K. Hartmann 1980. Near-infrared colorimetry of J6 Himalia and S9 Phoebe: A summary of 0.3- to 2.2- μm reflectances. *Icarus* **44**, 541–547.
- Dumas, C., R. J. Terrile, B. A. Smith, G. Schneider, and E. E. Becklin 1999. Stability of Neptune's ring arcs in question. *Nature* **400**, 733–735.
- Elias, J. H., J. A. Frogel, K. Matthews, and G. Neugebauer 1982. Infrared standard stars. *Astron. J.* **87**, 1029–1034.
- Fink, U., H. P. Larson, T. N. Gautier III, and R. R. Treffers 1976. Infrared spectra of the satellites of Saturn: Identification of water ice on Iapetus, Rhea, Dione, and Tethys. *Astrophys. J.* **207**, L63–67.
- Hahn, G., and C.-I. Lagerkvist 1988. Physical studies of asteroids. XVII. JHK photometry of selected main-belt and near-Earth asteroids. *Icarus* **74**, 454–471.
- Hartmann, W. K., D. P. Cruikshank, and J. Degewij 1982. Remote comets and related bodies: VJHK colorimetry and surface materials. *Icarus* **52**, 377–408.
- Jewitt, D., and J. Luu 1998. Optical-infrared spectral diversity in the Kuiper belt. *Astron. J.* **115**, 1667–1670.
- Karkoschka, E. 1997. Rings and satellites of Uranus: Colorful and not so dark. *Icarus* **125**, 348–363.
- Karkoschka, E. 1999. Small satellites of Uranus: Not so small, except the new one. *Bull. Am. Astron. Soc.* **31**, 1074.
- Kesten, P. R., J. K. Davies, D. Cruikshank, and T. L. Roush 1998. Uranian satellites and Triton: JHK photometry. *Bull. Am. Astron. Soc.* **30**, 1099–1100.
- Kuiper, G. 1949. The fifth satellite of Uranus. *Publ. Astron. Soc. Pacific* **61**, 129.
- Lun, J. X., and D. C. Jewitt 1998. Optical and infrared reflectance spectrum of Kuiper belt object 1996 TL₆₆. *Astrophys. J.* **494**, L117–120.
- Marchis, F., J. Berthier, P. Descamps, T. Fusco, R. Prange, and T. Sekiguchi 1999. Ground-based high resolution observations of the uranian system in the near IR. *Bull. Am. Astron. Soc.* **31**, 1074.
- Moroz, L. V., G. Arnold, A. V. Korochantsev, and R. Wäsch 1998. Natural solid bitumens as possible analogs for cometary and asteroid organics. 1. Reflectance spectroscopy of pure bitumens. *Icarus* **134**, 253–268.
- Morrison, D., D. P. Cruikshank, C. B. Pilcher, and G. H. Rieke 1976. Surface compositions of the satellites of Saturn from infrared photometry. *Astrophys. J.* **207**, L213–216.
- Nicholson, P. D. and T. J. Jones 1980. Two-micron spectrophotometry of Uranus and its rings. *Icarus* **42**, 54–67.
- Noll, K. S., J. Luu, and D. Gilmore 2000. Spectrophotometry of four Kuiper belt objects with NICMOS. *Astron. J.* **119**, 970–976.
- Owen, T. C., D. P. Cruikshank, C. M. Dalle Ore, T. R. Geballe, T. L. Roush, and C. de Bergh 1999. Detection of water ice on Saturn's satellite Phoebe. *Icarus* **139**, 379–382.

- Pascu, D., J. R. Rohde, P. K. Seidelmann, E. Wells, C. Kowal, A. Storrs, B. Zellner, D. G. Currie, and D. M. Dowling 1995. HST photometry of the uranian inner satellite system. *Bull. Am. Astron. Soc.* **27**, 1169–1170.
- Pascu, D., J. R. Rohde, P. K. Seidelmann, E. N. Wells, J. L. Hershey, B. H. Zellner, A. D. Storrs, D. G. Currie, and A. S. Bosh 1998a. HST BVI photometry of Triton and Proteus. *Bull. Am. Astron. Soc.* **30**, 1101.
- Pascu, D., J. R. Rohde, P. K. Seidelmann, E. N. Wells, C. T. Kowal, B. H. Zellner, A. D. Storrs, D. G. Currie, and D. M. Dowling 1998b. Hubble Space Telescope astrometric observations and orbital mean motion corrections for the inner uranian satellites. *Astron. J.* **115**, 1190–1194.
- Rayner, J. T., and 10 colleagues 1993. Design of a new 1–5.5 micron infrared camera for the NASA Infrared Telescope Facility. *Proc. SPIE* **1946**, 490–501.
- Roddiier, F., A. Brahic, C. Dumas, J. E. Graves, B. Han, M. J. Northcott, T. Owen, and C. Roddiier 1997a. Adaptive optics observations of solar systems objects. *Bull. Am. Astron. Soc.* **29**, 1023.
- Roddiier, F., C. Roddiier, A. Brahic, C. Dumas, J. E. Graves, M. J. Northcott, and T. Owen 1997b. First ground-based adaptive optics observations of Neptune and Proteus. *Planet. Space Sci.* **45**, 1031–1036.
- Roddiier, C., F. Roddiier, J. E. Graves, O. Guyon, and M. J. Northcott 1998a. *Satellites of Neptune*. IAU Circular 6987.
- Roddiier, C., F. Roddiier, J. E. Graves, O. Guyon, M. J. Northcott, and B. Sicardy 1998b. *Satellites and rings of Neptune*, IAU Circular 7051.
- Sagan, C., B. N. Khare, and J. S. Lewis 1984. Organic matter in the Saturn system. In *Saturn* (T. Gehrels and M. S. Matthews, Eds.), pp. 788–807. Univ. of Arizona Press, Tucson.
- Shure, M., D. W. Toomey, J. Rayner, P. Onaka, A. Denault, W. Stahlberger, D. Watanabe, K. Criez, L. Robertson, and D. Cook 1994. A powerful new infrared array camera for the NASA Infrared Telescope Facility. *Exp. Astron.* **3**, 239–242.
- Sicardy, B., F. Roddiier, C. Roddiier, E. Perozzi, J. E. Graves, O. Guyon, and M. J. Northcott 1999. Images of Neptune's ring arcs obtained by a ground-based telescope. *Nature* **400**, 731–733.
- Smith, B. A., and 10 colleagues 1986. Voyager 2 in the uranian system—Imaging science results. *Science* **233**, 43–64.
- Smith, B. A., and 63 colleagues 1989. Voyager 2 at Neptune—Imaging science results. *Science* **246**, 1422–1449.
- Soifer, B. T., G. Neugebauer, and K. Matthews 1981. Near-infrared spectrophotometry of the satellites and rings of Uranus. *Icarus* **45**, 612–617.
- Storrs, A. D., B. Zellner, E. N. Wells, B. Buratti, D. Currie, K. Seidelmann, and D. Pascu 1996. Spectrophotometry of small uranian satellites. *Bull. Am. Astron. Soc.* **28**, 1072.
- Sykes, M. V., B. Nelson, R. M. Cutri, J. D. Kirkpatrick, R. Hurt, and M. F. Skrutskie 2000. Near-infrared observations of the outer jovian satellites. *Icarus* **143**, 371–375.
- Terrile, R. J., C. Dumas, B. A. Smith, M. Rieke, G. Schneider, R. Thompson, E. Becklin, and D. Koerner 1998. First infrared imaging of the Neptune ring arcs: HST/NICMOS results. *Bull. Am. Astron. Soc.* **30**, 1044.
- Thomas, P. C. 1988. Radii, shapes, and topography of the satellites of Uranus from limb coordinates. *Icarus* **73**, 427–441.
- Thomas, P. C. 1989. The shapes of small satellites. *Icarus* **77**, 248–274.
- Thomas, P., and J. Veverka 1991. Neptune's small inner satellites. *J. Geophys. Res. Soc.* **96**, 19,261–19,268.
- Thomas, P., C. Weitz, and J. Veverka 1989. Small satellites of Uranus—Disk-integrated photometry and estimated radii. *Icarus* **81**, 92–101.
- Thomas, P. C., J. Veverka, and P. Helfenstein 1995. Neptune's small satellites. In *Neptune and Triton* (D. P. Cruikshank, Ed.), pp. 685–699. Univ. of Arizona Press, Tucson.
- Toomey, D. W., C. Ftaclas, R. H. Brown, and D. Trilling 1998. CoCo: An experiment in infrared coronagraphy at the IRTF. *Proc. SPIE* **3354**, 782–790.
- Veverka, J., P. Thomas, P. Helfenstein, R. H. Brown, and T. V. Johnson 1987. Satellites of Uranus—Disk-integrated photometry from Voyager imaging observations. *J. Geophys. Res.* **92**, 14,895–14,904.
- Wang, S.-I., P. D. Owensby, D. W. Toomey, R. H. Brown, W. E. Stahlberger, C. P. Cavedoni, R. Hua, and C. Ftaclas 1994. CoCo: An infrared cold coronagraph for astronomical observations. *Proc. SPIE* **2198**, 578–589.
- Weintraub, D. A., S. C. Tegler, and W. Romanishin 1997. Visible and near-infrared photometry of the centaur objects 1995 GO and 5145 Pholus. *Icarus* **128**, 456–463.
- Wilson P. D., C. Sagan, and W. R. Thompson 1994. The organic surface of 5145 Pholus: Constraints set by scattering theory. *Icarus* **107**, 288–303.